

Hydrodynamic View in the NICA Energy Range

V. Toneev^a and V. Skokov^a

^a *Joint Institute for Nuclear Research, 141980 Dubna, Moscow Region, Russia*

Abstract

Results for penetrating probes treated within a hybrid hydro-kinetic model are projected onto the energy range covered by the NICA and FAIR projects. A new source of dileptons emitted from a mixed quark-hadron phase, quark-hadron bremsstrahlung, is proposed. An estimate for the $\pi\pi \rightarrow \sigma \rightarrow \gamma\gamma$ process in nuclear collisions is given.

D.I. Blokhintsev, whose centennial anniversary of the birthday this conference is devoted to, has contributed to various fields of physics and its applications, particularly, to hydrodynamics. Sixteen years ago, at the dawn of hydrodynamics he made an important remark [1] concerning possible violation of the uncertainty principle in initial conditions of the Landau hydrodynamic theory. From up-to-date view, this Blokhintsev's estimate looks slightly naive but in principle it is correct until now and should be taken into account in modern development of a relativistic hydrodynamic approach. Here we present a hybrid model which combines kinetic and hydrodynamic descriptions. To certain extent it can be considered as a possible solution of the problem put by D.I. Blokhintsev.

In the hybrid model [2], the initial stage of heavy ion collisions is treated kinetically within the transport Quark Gluon String Model (QGSM) [3] whereas the subsequent stage is considered as an isentropic expansion of a formed dense and hot system (fireball). The transition from one stage to another is solved by considering the entropy evolution.

In Fig.1, the ratio between entropy S and baryon charge Q_B of participants is shown for In+In collisions at the impact parameter $b = 4$ fm and bombarding energy 158 AGeV. Being calculated on a large 3D grid, this ratio is less sensitive to particle fluctuation as compared to the entropy itself. Small values of the baryon charge Q_B at the very beginning of collision result in large values of the S/Q_B ratio. It is clearly seen that for $t_{kin} \gtrsim 1.3$ fm/ c this ratio is practically constant and this stage may be considered as isentropic expansion.

To proceed from kinetics to hydrodynamics, we evaluate conserved components of the energy-momentum tensor $T_{00}, T_{01}, T_{02}, T_{03}$ and baryon density n_B (the zero component of the baryon current) within QGSM at the moment $t_{kin} = 1.3$ fm/ c in every cell on the 3D grid. This state is treated as an initial state for subsequent hydrodynamic evolution of a fireball. The time dependence of average thermodynamic quantities is presented in the left panel of Fig.1.

The latter stage is evaluated within the relativistic 3D hydrodynamics [2]. The key quantity is the equation of state. In this work, the mixed phase Equation of State (EoS) is applied [5] which allows for coexistence of hadrons and quarks/gluons. This thermodynamically consistent EoS uses the modified Zimanyi mean-field interaction for hadrons and also includes interaction between hadron and quark-gluon phases, which results in a crossover deconfinement phase transition. In addition to [5], the hard thermal loop term was self-consistently added to the interaction of quarks and gluons to get the correct asymptotics

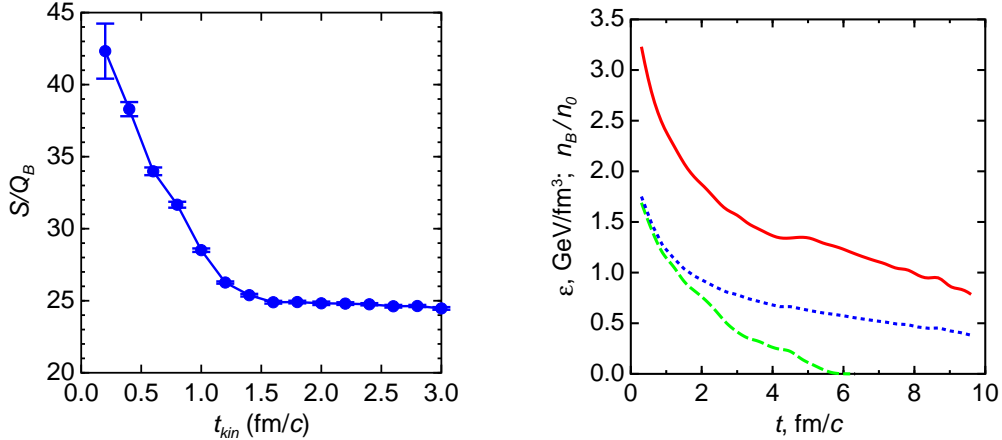


Figure 1: Temporal dependence of entropy S per baryon charge Q_B of participants (left panel) for a semi-central In+In collision at $E_{lab} = 158$ AGeV. In the right panel the average energy (solid line) and baryon (dashed) densities of an expanding fireball formed in this collision. Dotted line shows a contribution of quarks and gluons to the energy density.

at $T \gg T_c$ and reasonable agreement of the model results with lattice QCD calculations at finite temperature T and chemical potential μ_B [6]. This agreement is demonstrated in Fig.2 where the reduced pressure $\Delta p/T^4 = (p(\mu_B) - p(\mu_B = 0))/T^4$ is compared with recent lattice QCD data.

The fraction of unbound quarks/gluons defined as $\rho_{pl}/\rho = (n_q + n_{\bar{q}} + n_g)/(n_q + n_{\bar{q}} + n_g + n_B + n_M)$ is presented for the mixed phase EoS in the right panel of Fig.2. It is seen that even at a moderate temperature $T \sim 50 \div 100$ MeV the quark/gluon fraction sharply increases at the baryon density $n_B/n_0 \sim 6$ and dominates thereafter. At $T = 200$ MeV the admixture of hadrons is, naturally, quite small.

Consider now penetrating probes. To find observable dilepton characteristics, one should integrate the emission rate over the whole time-space $x \equiv (t, \mathbf{x})$ evolution, add the contribution from the freeze-out surface ('hadron cocktail'), and take into account the experimental acceptance. To simplify our task, we consider only the main channel $\pi\pi \rightarrow \rho \rightarrow l^+l^-$. In this case the dilepton emission rate is

$$\frac{d^4 R^{l^+l^-}}{dq^4} = - \int d^4x \mathcal{L}(M) \frac{\alpha^2}{\pi^3 q^2} f_B(q_0, T(x)) \text{Im}\Pi_{em}(q, T(x), \mu_b(x)) , \quad (1)$$

where the integration is carried out over the whole space grid and time from $t = 0$ till the local freeze-out moment. Here $q^2 = M^2 = q_0^2 - \mathbf{q}^2$, $f_B(q_0, T(x))$ is the Bose distribution function, and $\mathcal{L}(M)$ is the lepton kinematic factor. The imaginary part of the electro-magnetic current correlation function $\text{Im}\Pi_{em}(q, T(x), \mu_b(x))$ includes in-medium effects which may be calculated in different scenarios. The recent precise measurements of muon pairs [7] allowed one to discriminate two main scenarios, in particular those based on the Brown-Rho (BR) scaling hypothesis [8] assuming a dropping ρ mass and on a strong broadening of ρ -meson spectral function as found in the many-body approach by Rapp and Wambach [9]. It was shown [7] that the measured excess of muons is nicely described by the strong broadening of the ρ -meson spectral function. In contrary, the BR scaling hypothesis predicts a large shift of the ρ -meson maximum towards lower invariant mass M in contradiction with

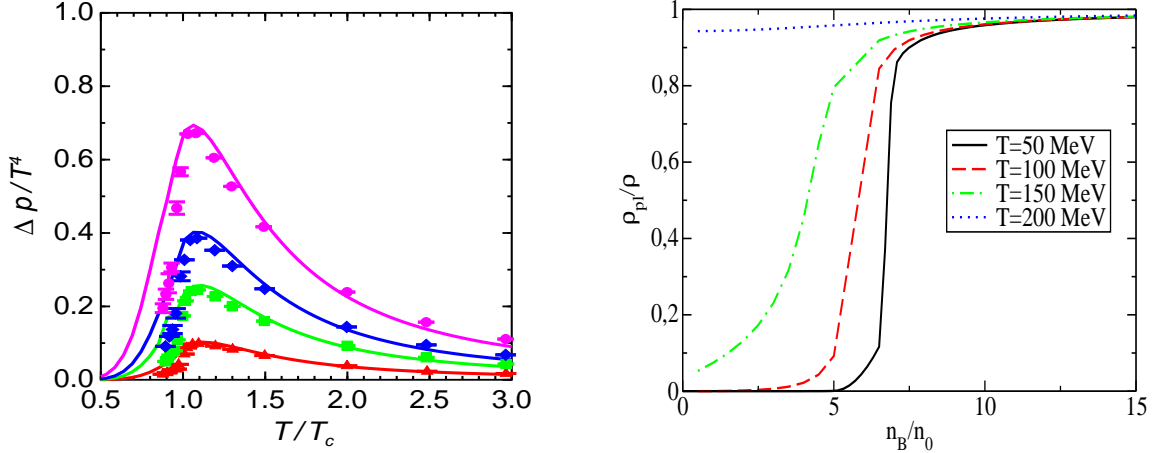


Figure 2: Temperature dependence of the reduced pressure (left panel) at the baryon chemical potential $\mu_B = 210, 330, 410$ and 530 MeV (from the bottom) and fraction of unbound quarks (right panel) within the mixed phase EoS. Points are lattice QCD data for the 2+1 flavor system [6].

experimental data [7].

This result looks quite disappointing. First, one sees no signal of a partial restoration of the chiral symmetry for the sake of which dilepton measurements were originally undertaken. Second, to be consistent with the QCD sum rules *both* collision broadening *and* ρ -mass dropping should be taken into account [10]. Generally, the exact relation between the ρ mass and quark condensate is not fixed by the QCD sum rules in contrast with the BR scaling, so it is questionable whether to prescribe some T dependence to the BR mass shift. This shortcomings of the analysis in [7] are commented by Brown and Rho [11]. In this respect, for the pion annihilation $\pi\pi \rightarrow \rho \rightarrow \mu^+\mu^-$ we estimated [2] the imaginary part of the ρ -meson self-energy in the one-loop approximation assuming the Hatsuda-Lee relation for the modified ρ mass: $m_\rho^*(x) = m_\rho(1 - 0.15 \cdot n_B(x)/n_0)$. The calculated result is presented in Fig.3 by the solid line [2]. Indeed, the shift of the ρ -meson spectral function is not so drastic as in [7]. In addition, one should note that dileptons carry direct information on the ρ meson spectral function only if the vector dominance is valid [11]. It is not the case in the Harada-Yamawaki vector manifestation of hidden local symmetry [12].

As seen from Fig.3, the muon yield is underestimated at both low and high values of the $\mu^+\mu^-$ invariant mass M . In the broadening scenario a low M component is explained by particle-hole excitations but not a partial chiral symmetry restoration. However, the existence of the mixed quark-hadron phase, those study is the main aim of the Nuclotron-based Ion Collider fAcility (NICA) project [13], may give rise to a new dilepton source, quark(antiquark)-hadron bremsstrahlung. Similarly to the np bremsstrahlung, the process for an antiquark-hadron collision may roughly be estimated in the soft-photon approximation as

$$\frac{dN_{qN}^{l+l^-}}{dM^2}(s, M) \approx K \frac{\alpha^2}{3\pi^2} \frac{\bar{\sigma}(s)}{M^2} \ln \left[\frac{s^{1/2} - m_N - m_q}{M} \right]. \quad (2)$$

Here the averaged cross section $\bar{\sigma}(s) = \sigma_{el}^{qN} [s/(m_N + m_q)^2 - 1]$ and the elastic qN cross

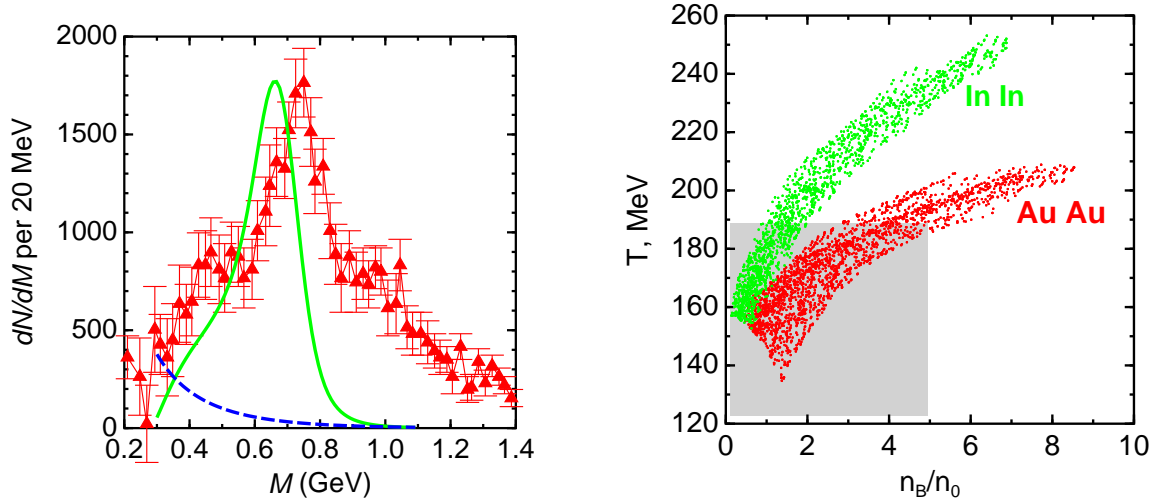


Figure 3: Invariant mass distribution of dimuons (left panel) from semi-central In+In collisions at the beam energy 158 AGeV. Experimental points are from [7]. The solid line corresponds to the T -independent dropping mass [2] and the dashed one is the contribution of the quark-hadron bremsstrahlung channel. In the right panel one compares dynamical trajectories projected onto the $T - n_B$ plane for central In+In(158 AGeV) and Au+Au(40 AGeV). The shaded region roughly corresponds to the hadronic phase.

section is approximated by the quark scaled NN cross section [14]

$$\sigma_{el}^{qN} = \left[\frac{18m_N(mb \cdot GeV^2)}{s - (m_N + m_q)^2} - 10 (mb) \right] \times \frac{1}{3}. \quad (3)$$

So the production rate will be

$$\frac{dN_{qN}^{l^+l^-}}{dM^2} = \int d^4x \int \frac{d^3k_q}{(2\pi)^3} f(\mathbf{k}_q, T(x)) \int \frac{d^3N_q}{(2\pi)^3} f(\mathbf{k}_N, T(x)) \frac{dN_{qN}^{l^+l^-}}{dM^2}(s, M) v_{rel}, \quad (4)$$

where v_{rel} is the relative velocity of colliding qN particles and the integration in (4) should be carried out over the whole space-time available for the mixed phase. The free mass is used for a nucleon and $m_q = 150$ MeV for an antiquark. In a real case one should also add contributions from all other baryons, as well as that from quark-antibaryon and quark(antiquark)-meson interactions with proper cross sections. All these uncertainties are effectively introduced in (2) by an arbitrary factor K .

As follows from the dashed line in Fig.3, at rather reasonable value of $K = 10$ the qN bremsstrahlung source improves agreement with experiment. It is of interest that the contribution of this new source decreases when the bombarding energy goes down till the NICA energy range (≤ 40 AGeV) while the contribution from particle-hole excitation is expected to grow since the baryon density in this range is higher (see below) allowing, in principle, disentangling of these two sources. The underestimated yield at high M , intermediate mass dileptons, can mainly be described by Drell-Yan process in the quark phase [15]. The mixed quark-hadron phase should also contribute to the intermediate M region. Its contribution can be taken into account in the way as the Drell-Yan process

with an additional hadron form factor. Effectively, it will increase the Drell-Yan lepton yield [15].

The phase distribution of all space cells at the early evolution moment $t = 0.3$ fm/c projected on the $T - n_B$ plane is presented in Fig.3. It is seen that at the maximal NICA energy the baryon density in the hadronic phase for central Au+Au collisions is noticeably higher than that at the SPS energy in In+In collisions. It means that the difference between the BR scaling and broadening scenarios is expected to be more pronounced at the NICA energy.

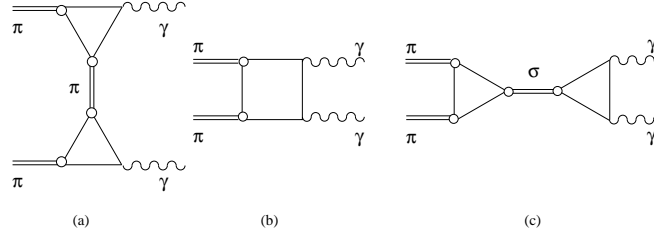


Figure 4: Quark diagrams for the 2γ production in the Born approximation (a), (b) and through the σ resonance (c).

Annihilation of two pions into two photons is of particular interest since its cross section is sensitive to changes of the σ -meson properties which occur in the vicinity of chiral restoration phase transition. With increasing temperature and density the σ meson changes its character from a broad resonance with a large decay width into two pions to a bound state below the two-pion threshold $m_\sigma(T, \mu_B) \lesssim 2m_\pi(T, \mu_B)$. The calculation of the photon pair production rate at the given T as a function of the invariant mass shows a strong enhancement and narrowing of the σ resonance at the threshold due to chiral symmetry restoration [16]. We make the first estimate of this channel for a particular nuclear collision.

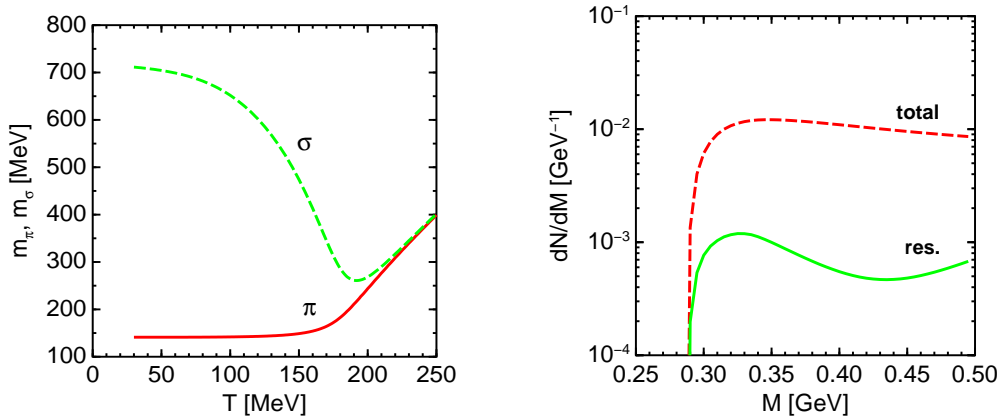


Figure 5: T-dependence of σ and π masses (left panel) and total (dashed line) and resonance (solid line) invariant mass distributions of two photon pairs created in the central Au+Au collision at 40 AGeV (right panel).

In-medium $\pi\pi \rightarrow \gamma\gamma$ process is evaluated within the NJL model [16]. Besides the resonance diagram, the dominating Born terms are considered, see Fig.4. So the total rate has the Born term, resonance term and interference between them: $dN_{tot}^{\gamma\gamma}/dM^2 = dN_{Born}^{\gamma\gamma}/dM^2 + dN_{res}^{\gamma\gamma}/dM^2 + dN_{interf}^{\gamma\gamma}/dM^2$ which should be substituted in eq.(4).

The temperature dependence of σ and π masses for this model is shown in Fig.5. The regime $m_\sigma(T, \mu_B) < 2m_\pi(T, \mu_B)$ starts at $T \sim 165$ MeV. The photon yield as a function of photon pair invariant mass is presented in Fig.5 for central Au+Au collisions at 40 AGeV. The total number of photon pairs sharply increases above the threshold $2m_\pi$ and then flattens on the level of $\sim 10^{-2}$. The resonance channel of interest is lower by about the order of magnitude as compared to the total yield and exhibits a spread weak maximum. The maximum predicted in [16] for the fixed T is washed out, as seen from Fig.5. It is not an easy but promising experimental problem to select out this maximum from the total distribution. Note that such an analysis should be carried out on a huge background of γ decays of 'hadron cocktail'.

One of the authors (V.T.) is deeply indebted to D.I. Blokhintsev who many years ago brought him into physics of high-energy interactions. We are thankful to E. Kolomeitsev for valuable remarks. This work was supported in part by the Deutsche Forschungsgemeinschaft (DFG project 436 RUS 113/558/0-3), the Russian Foundation for Basic Research (RFBR grants 06-02-04001 and 08-02-01003), special program of the Ministry of Education and Science of the Russian Federation (grant RNP.2.1.1.5409).

References

- [1] D.I. Blokhintsev, JETP **32**, 350 (1957).
- [2] V.V. Skokov and V.D. Toneev, Phys. Rev. **C73**, 021902 (2006); Acta Physica Slovaca **56**, 503 (2006).
- [3] N.S. Amelin, K.K. Gudima, S.Y. Sivoklov and V.D. Toneev, Sov. J. Nucl. Phys. **52**, 172 (1990); N.S. Amelin, E.F. Staubo, L.P. Csernai, V.D. Toneev and K.K. Gudima, Phys. Rev. C **44**, 1541 (1991); V.D. Toneev, N.S. Amelin, K.K. Gudima and S.Yu. Sivoklov, Nucl. Phys. **A519**, 463c (1990).
- [4] V.V. Skokov and V.D. Toneev, Sov. J. Nucl. Phys. **70**, 109 (2007).
- [5] V.D. Toneev, E.G. Nikonov, B. Friman, W. Nörenberg, and K. Redlich, Eur. Phys. J. **C32**, 399 (2004).
- [6] Z. Fodor, Nucl. Phys. A **715**, 319 (2003); F. Csikor, G.I. Egri, Z. Fodor, S.D. Katz, K.K. Szabo, and A.I. Toth, JHEP **405**, 46 (2004).
- [7] NA60 Collaboration, Phys. Rev. **96**, 162302 (2006); Nucl. Phys. **A774**, 715 (2006).
- [8] G.E. Brown and M. Rho, Phys. Rev. Lett. **66**, 2720 (1991).
- [9] R. Rapp and J. Wambach, Adv. Nucl. Phys. **25**, 1 (2000); R. Rapp, G. Chanfray and J. Wambach, Phys. Rev. Lett. **76**, 368 (1996)
- [10] J. Ruppert, T. Renk and B. Muller, Phys. Rev. **C73**, 034903 (2006).
- [11] G.E. Brown and M. Rho, nucl-th/0509001, nucl-th/0509002.
- [12] M. Harada and K. Yamawaki, Phys. Repts. **381**, 1 (2003).
- [13] NICA project: <http://nica.jinr.ru>.
- [14] C. Gale and J. Kapusta, Phys. Rev. **C35**, 2107 (1987).
- [15] C.M. Hung and E.V. Shuryak, K. Dusling, Phys. Rev. **C56**, 453 (1997); D. Teaney and I. Zahed, Phys. Rev. **C75**, 024908 (2007); H. van Hees and Rapp, arXiv:0711.3444.
- [16] M.K. Volkov, E.A. Kuraev, D. Blaschke, G. Röpke and S. Schmidt, Phys. Lett. **B424**, 235 (1998).